Electronic Supplementary Information

for

Investigations of the interactions between ZnO nanorods and H_2 with ^{17}O NMR spectroscopy

Benteng Song,[†a] Fang Wang,[†b] Qin Zhu,[†b] Ling-Hai Xie,[a] Luming Peng[*b]

[a] Key Laboratory for Organic Electronics and Information Displays (KLOEID) & Institute of Advanced Materials (IAM), Jiangsu National Synergetic Innovation Center for Advanced Materials (SICAM), Nanjing University of Posts & Telecommunications, 9 Wenyuan Road, Nanjing 210023, China

[b] Key Laboratory of Mesoscopic Chemistry of Ministry of Education and Collaborative Innovation Center of Chemistry for Life Sciences, School of Chemistry and Chemical Engineering, Nanjing University, Nanjing 210023, China

[†] These authors contributed equally.

[*] Correspondence: luming@nju.edu.cn

Contents

1. Material preparation

ZnO nanorods were prepared by hydrothermal pathway.[1] In detail, 1.6 mmol of $Zn(Ac)_2 \cdot 2H_2O$ and 3.2 mmol of NaOH were dissolved in 80 mL of ethanol respectively. The NaOH solution was then mixed with $Zn(Ac)_2$ solution under constant agitation, subsequently, 0.19 g of ethanediamine (EDA) reagent was added to above mixed solution. After 0.5 h with stirring, above mixed solution was transferred to Teflon-lined autoclave, then heated at 160 °C for 8 h. The white precipitate was centrifuged five times with distilled water. Finally, ZnO samples were obtained after dried (80 °C for 8 h).

2. Material characterization

The powder XRD experiment was performed on a Philips X'Pro X-ray diffractometer operated at 40 mA and 40 kV at room temperature. The morphology of ZnO was obtained using a JEOL JEM-2010 type electron microscope. A Bruker EMX-10/12 spectrometer was used to record EPR spectra of ZnO nanorods at 25 °C. XPS spectra of the samples exposing to H_2 were obtained on a Thermo Scientific EscaLab 250Xi.

3. ^{17}O isotopic labeling

ZnO nanorods were surface-selectively labeled with 90% ^{17}O-enriched H_2O (Cambridge Isotope Laboratories). The sample was first activated in a glass tube under vacuum at 100 °C for 2 h. After it was cooled to ambient temperature, $H_2{}^{17}O$ vapor was introduced through the vacuum line. The mixture was heated at 40 °C for 5 h before it was dried under vacuum.

4. Hydrogen activation

The ZnO nanorods labeled with $H_2{}^{17}O$ were heated at H_2 activation temperature under vacuum to remove surface adsorbed water. Then 500 mbar H_2 was supplied to ZnO sample in a sealed quartz tube and heated at different temperatures to study the interaction between ZnO and H_2.

5. Solid-state NMR spectroscopy

Solid-state NMR experiments were acquired at room temperature on 9.4 T Bruker Avance III spectrometers. ZnO samples were packed into 4.0 mm MAS probes double, the corresponding radiofrequency fields were tuned to ^{17}O and ^{1}H nuclei at 54.2 and 400 MHz, respectively. Chemical shifts for ^{17}O and ^{1}H are referenced to H_2O and adamantane at 0.0 and 1.79 ppm, respectively.

6. DFT calculations

In this section, the calculated parameters for H_2 adsorption and dissociation on ZnO surface are the same as our previous work.[2]

7. Characterization of ZnO nanomaterials

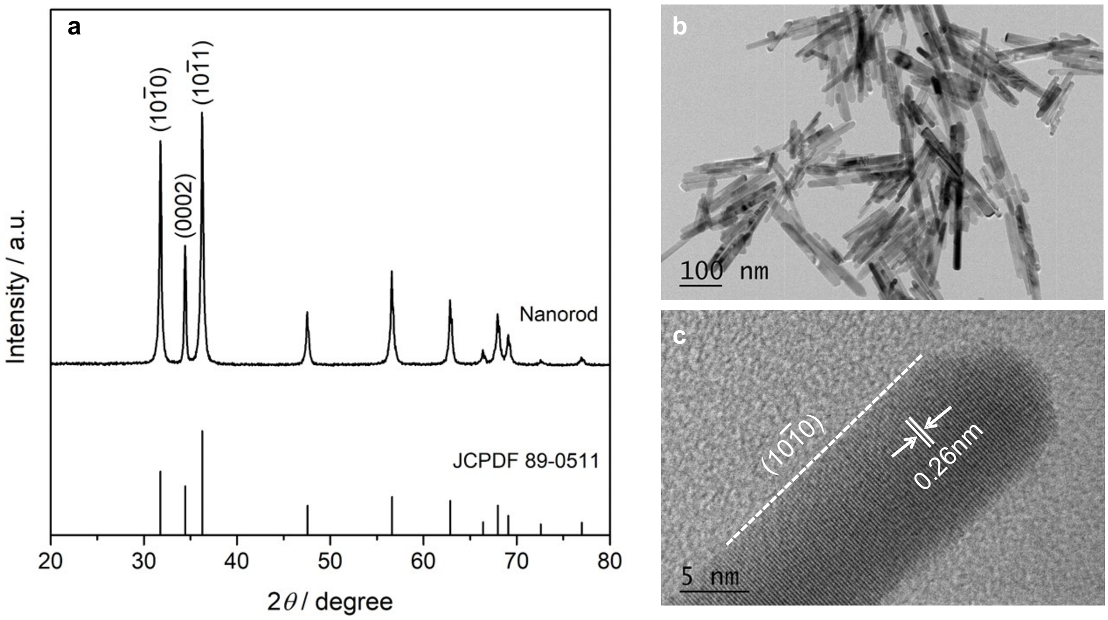

Fig. S1 (a) XRD pattern and (b) TEM, (c) HRTEM images of ZnO nanorods.

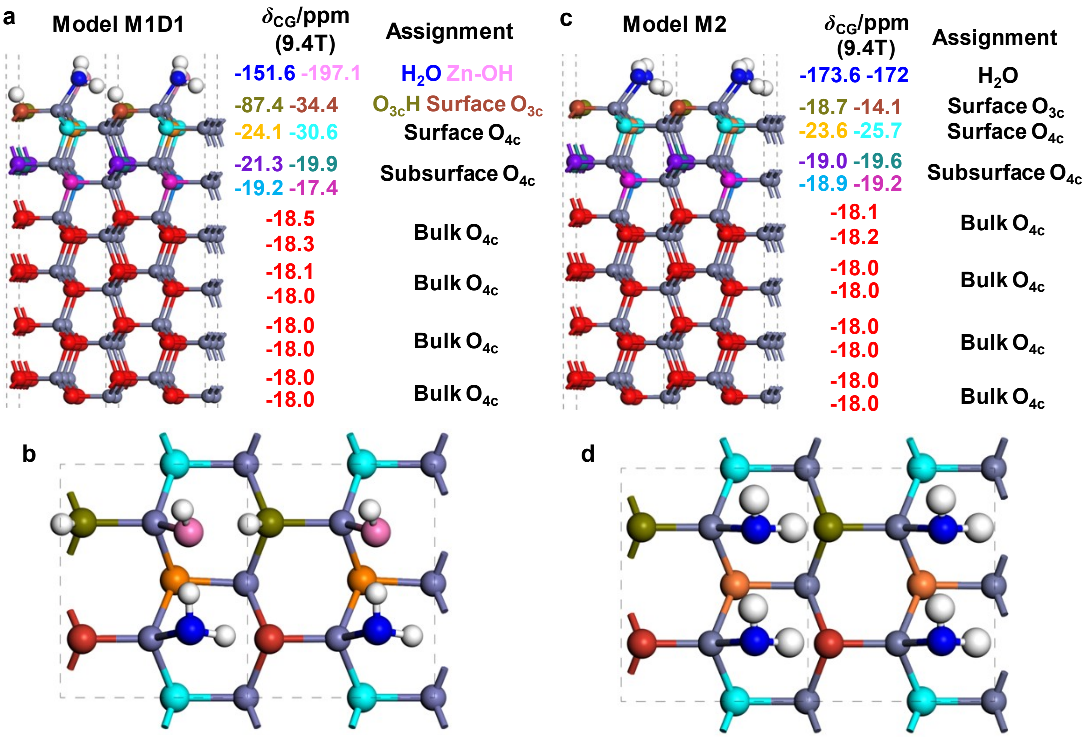

Fig. S2 The structural models of ZnO nanorods used for DFT calculations. (a) (Side view), (b) (Top view) The optimized ZnO $(10\bar{1}0)$ surface with a monolayer of water molecules in which half of the water molecules are dissociatively adsorbed, while the other half molecularly adsorbed (model M1D1); (c) (Side view), (d) (Top view) ZnO $(10\bar{1}0)$ surface with a monolayer of molecularly adsorbed water molecules (model M2).

The surface and subsurface oxygen species can be conveniently assigned according to the DFT calculation results. The observed disparity in NMR shifts (δ_{CG}) between surface OH and H_2O, when compared to the calculated values, can be attributed to the chosen calculation method, specifically the inclusion of Hubbard *U* corrections.[2]

Table S1. The assignments of different ^{17}O signals of ZnO nanorods obtained at 9.4 T.[2]

^{17}O shift/ppm	**Assignment**
-18.5	Bulk O_{4c}
-18.8 (broad)	Surface O_{3c} (M2)
-18.8 (narrow)	Subsurface O_{4c}
-24.7	Surface O_{4c}
-29.5	Surface O_{4c}
~ -34	Surface O_{3c} (M1D1)
~ -52	OH

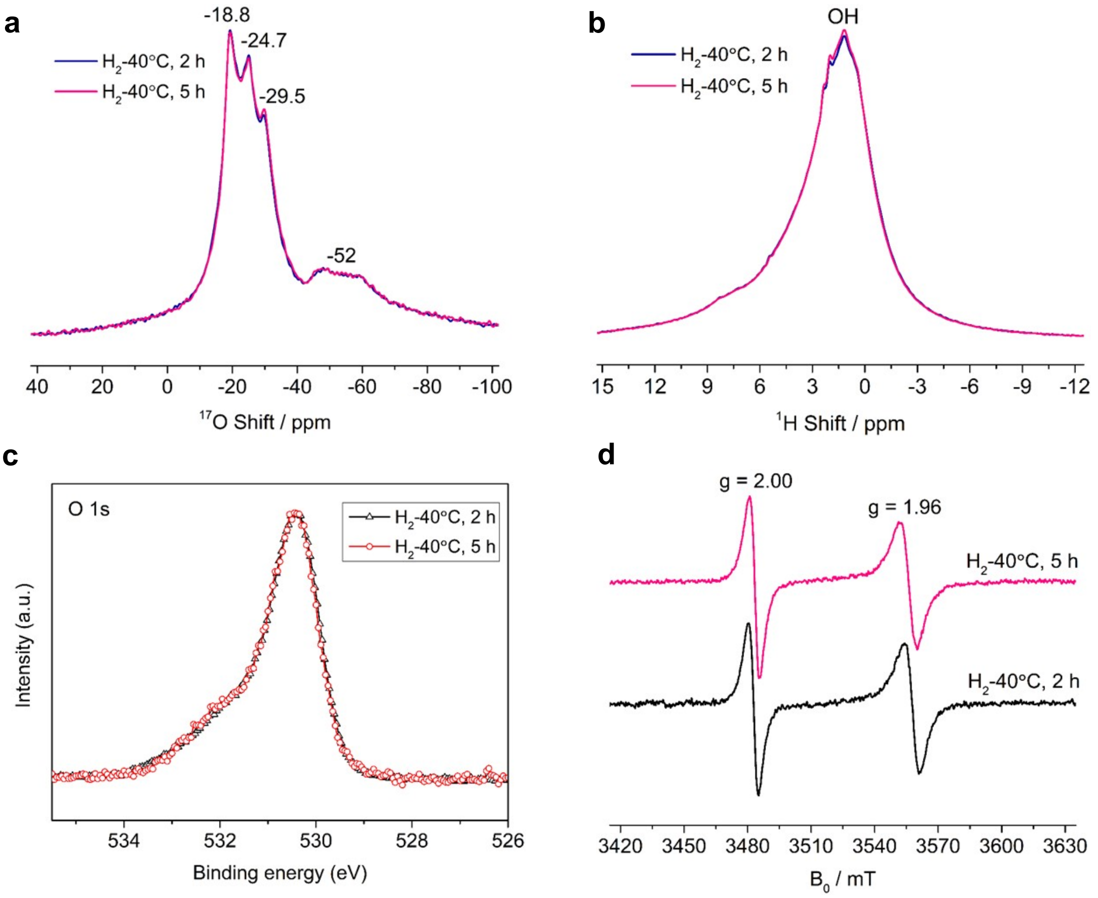

Fig. S3 (a) ^{17}O and (b) ^{1}H MAS NMR spectra of ZnO nanorods after exposing to H_2 (500 mbar) at 40 °C for 2 h and 5 h, respectively, and the corresponding (c) O 1s XPS spectra and (d) EPR spectra of ZnO nanorods. Where the signal at g = 2.00 corresponds to unpaired electrons trapped in oxygen vacancies, another signal at g = 1.96 represents unpaired electrons trapped from the conductive band by shallow donors or impurities.[3]

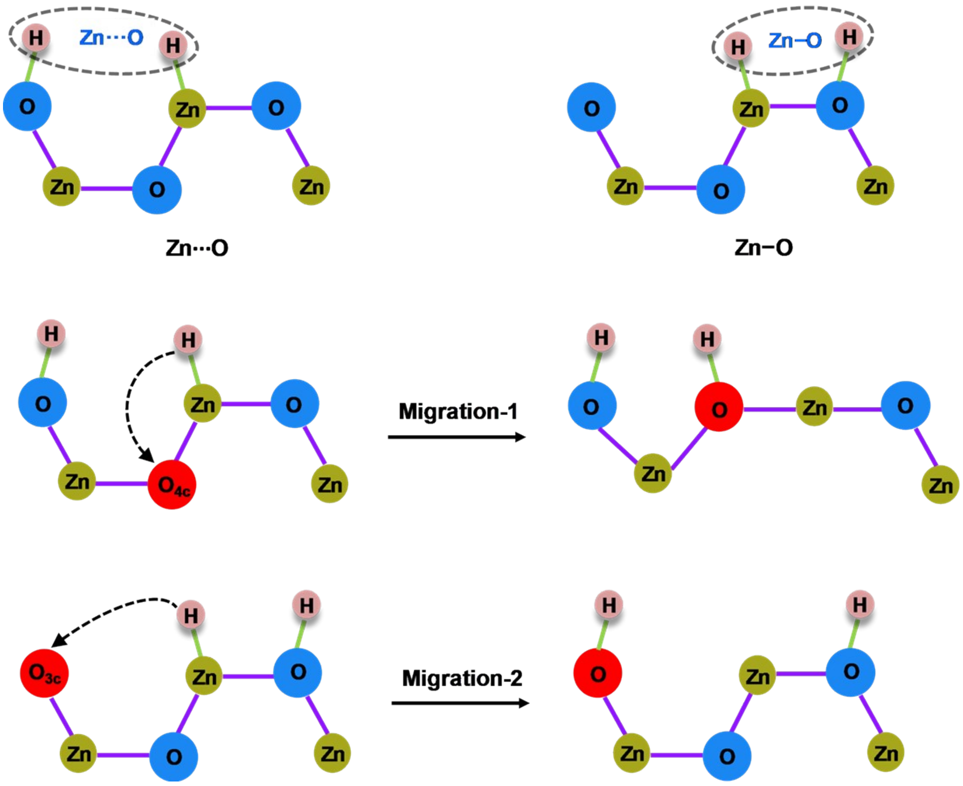

Fig. S4 Schematic diagram for the H_2 activation mechanisms on ZnO nanorods. ‘Zn···O ’ and ‘Zn−O’ represent heterolytic dissociation of H_2 at surface O_{3c} and Zn_{3c} sites, both of which generate an O-H (hydroxyl) and a Zn-H (hydride) site. ‘Migration-1’ and ‘Migration-2’ represent migration process of the formed Zn-H species to nearby surface O_{4c} and O_{3c} sites, respectively.

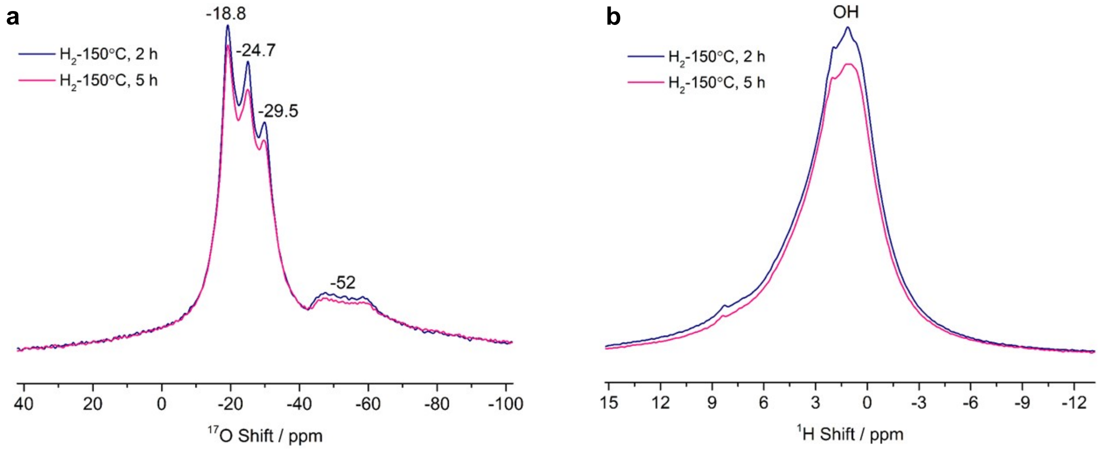

Fig. S5 ^{17}O and ^{1}H MAS NMR spectra of ZnO nanorods after exposing to H_2 (500 mbar) at 150 °C for 2 h and 5 h.

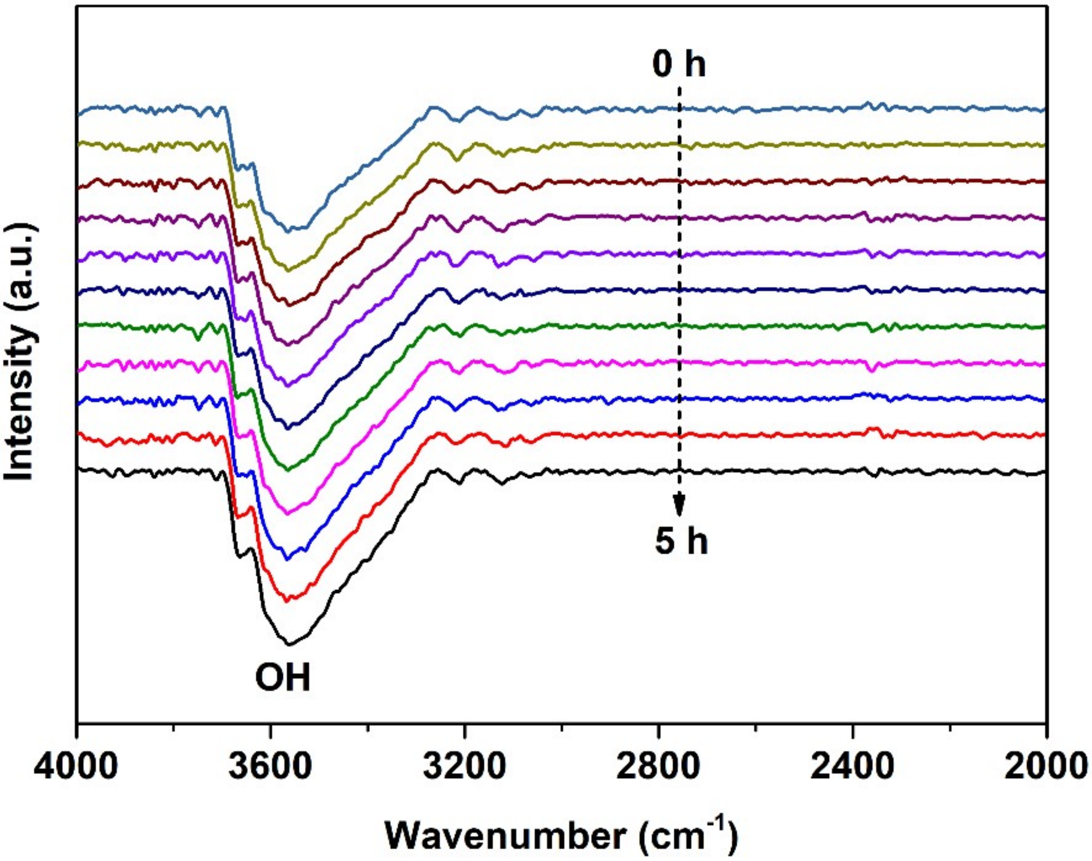

Fig. S6 In situ FT-IR spectra of ZnO nanorods at 150 °C in H_2 (99.9 % H_2) flow.

Table S2. The calculated energy for H_2 dissociation on ZnO($10\bar{1}0$) facets through the heterolytic pathways.[2] The corresponding structures are shown in Fig. 2 and Fig. S4.

Heterolytic pathways	Energy barrier / eV	Adsorption energy / eV
Zn···O	0.19	-0.24
Zn−O	0.54	-0.48
Zn···O···$O_V(O_{3c})$	0.58	0.09
Zn−O···$O_V(O_{3c})$	0.54	-0.42
Zn···O···$O_V(O_{4c})$	0.27	-0.38
Zn−O···$O_V(O_{4c})$	0.57	-0.42

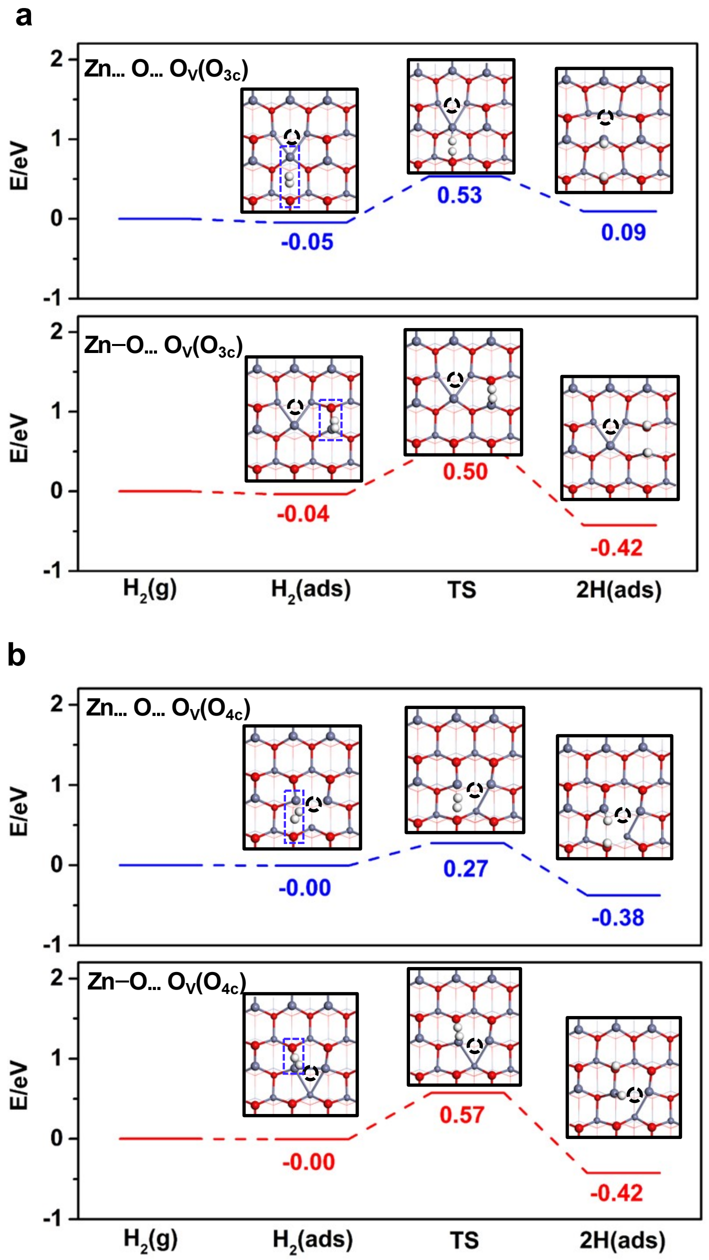

Fig. S7 The corresponding structures for H_2 adsorption on ZnO surface shown in Fig. 2. (a) Heterolytic dissociation of H_2 at surface O_{3c} and Zn_{3c} sites close to oxygen vacancy (originally O_{3c}). (b) Heterolytic dissociation of H_2 at surface O_{3c} and Zn_{3c} sites close to oxygen vacancy (originally O_{4c}). “TS” represents transition states. The dashed circles represent oxygen vacancy (O_V). The blue dashed rectangles indicate the Zn and O sites participating in H_2 dissociation. Oxygen, zinc, and hydrogen are in red, gray, and white, respectively.

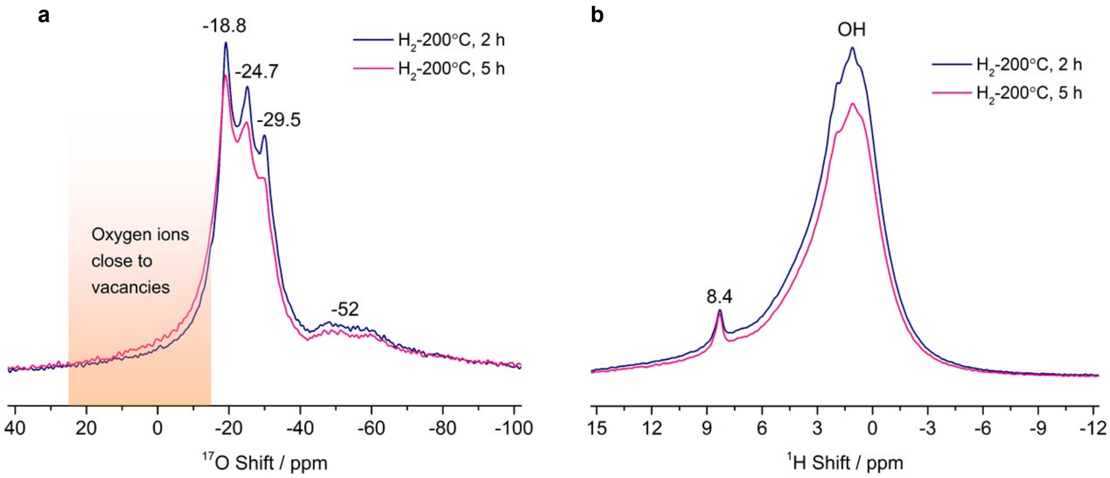

Fig. S8 ^{17}O and ^{1}H MAS NMR spectra of ZnO nanorods after exposing to H_2 (500 mbar) at 200 °C for 2 h and 5 h. The intensity of the high-frequency shoulder (~-15 to 25 ppm) related to surface oxygen vacancy becomes stronger in ^{17}O NMR spectra after exposing to H_2 5 h compared to the samples with H_2 exposure time of 2 h, owing to a relatively strong reduction reaction for ZnO nanorods.

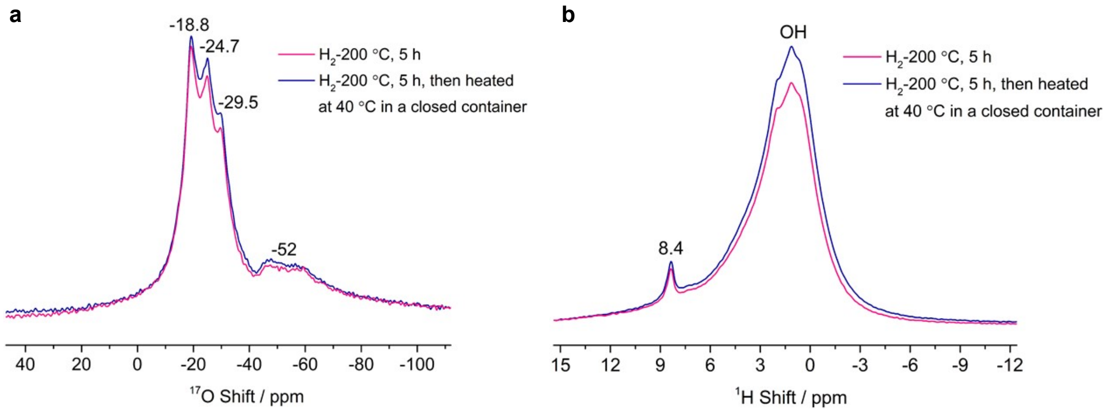

Fig. S9 ^{17}O and ^{1}H MAS NMR spectra of ZnO nanorods after exposing to H_2 (500 mbar) at 200 °C for 5 h and ZnO nanorods after being heated at 40 °C in a closed container.

For comparison, the spectral intensities for the peaks at -18.8, -24.7, -29.5 and -52 ppm are stronger in the ^{17}O NMR spectrum of ZnO nanorods heated at 40 °C in a closed container after exposing to H_2 at 200 °C, suggesting that some water molecules generated in the reduction process are adsorbed on the ZnO surface again, possibly reacting with oxygen vacancies to form surface hydroxyls, which is further supported by the change of spectral intensity in ^{1}H NMR of ZnO nanorods with and without heated at 40 °C in a closed container after exposing to H_2 at 200 °C.

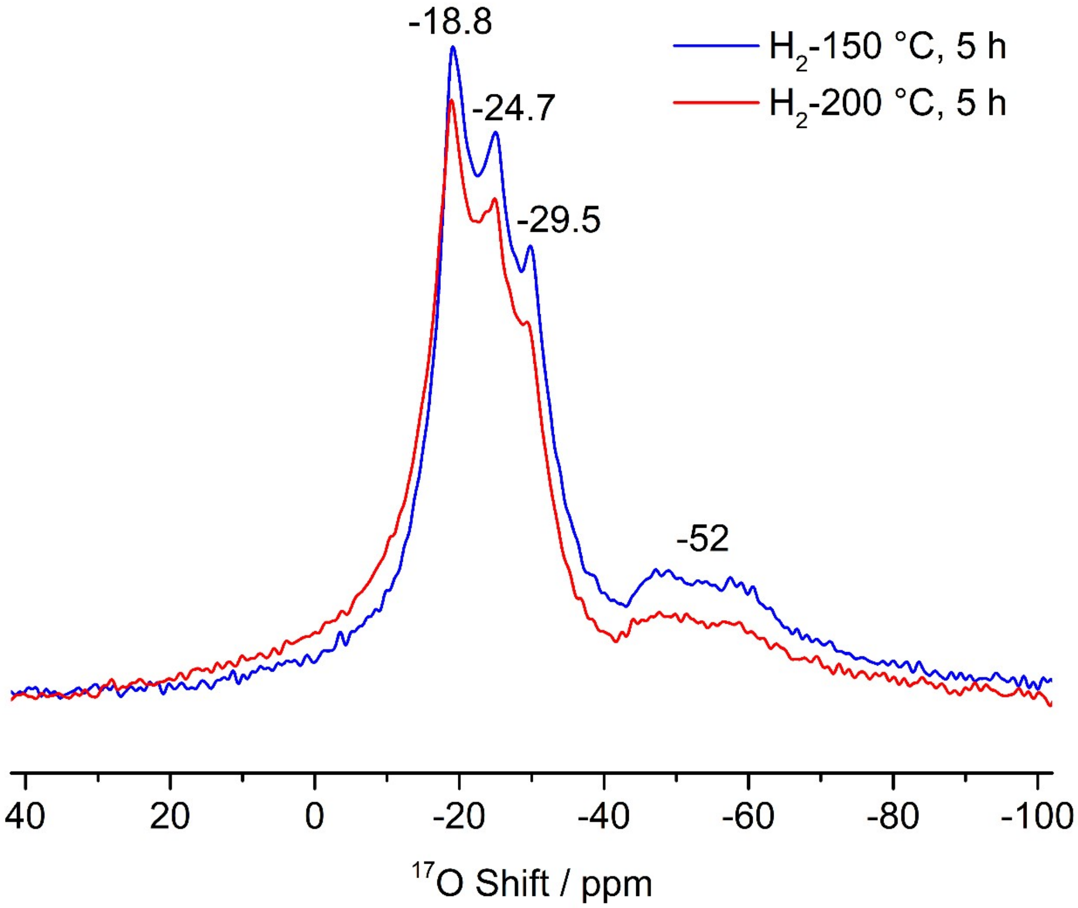

Fig. S10 ^{17}O MAS NMR spectra of ZnO nanorods after exposing to H_2 (500 mbar) at 150 °C and 200 °C, respectively.

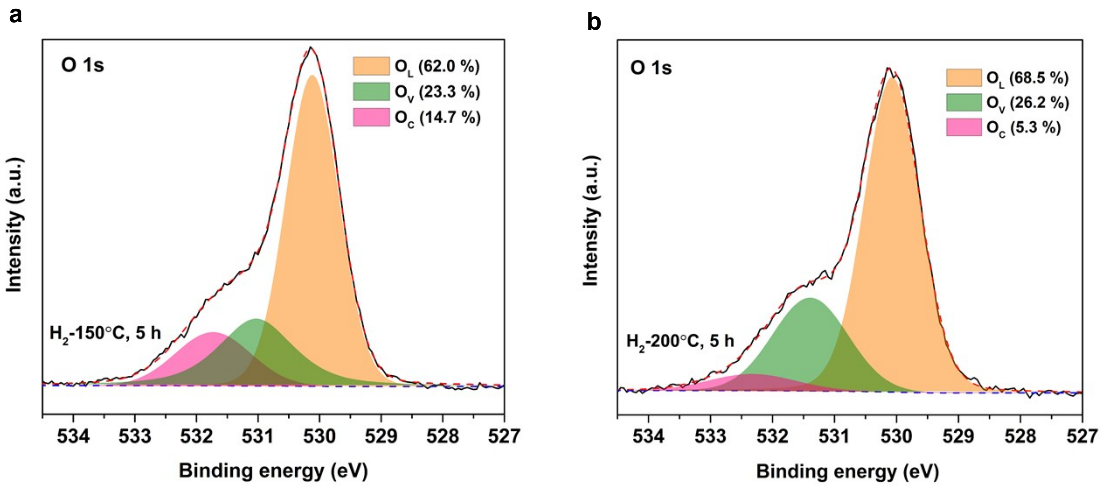

Fig. S11 O 1s XPS spectra of ZnO nanorods after exposing to H_2 (500 mbar) at 150 °C and 200 °C, respectively.

Table S3. The fractions of different oxygen species in O 1s XPS spectra of ZnO nanorods after exposing to H_2 (500 mbar) at 200 °C and 300 °C.

Sample	Fraction / %		
	O_L	O_V	O_C
H_2-200 °C, 5h	68.5	26.2	5.3
H_2-300 °C, 5h	69.5	23.1	7.4

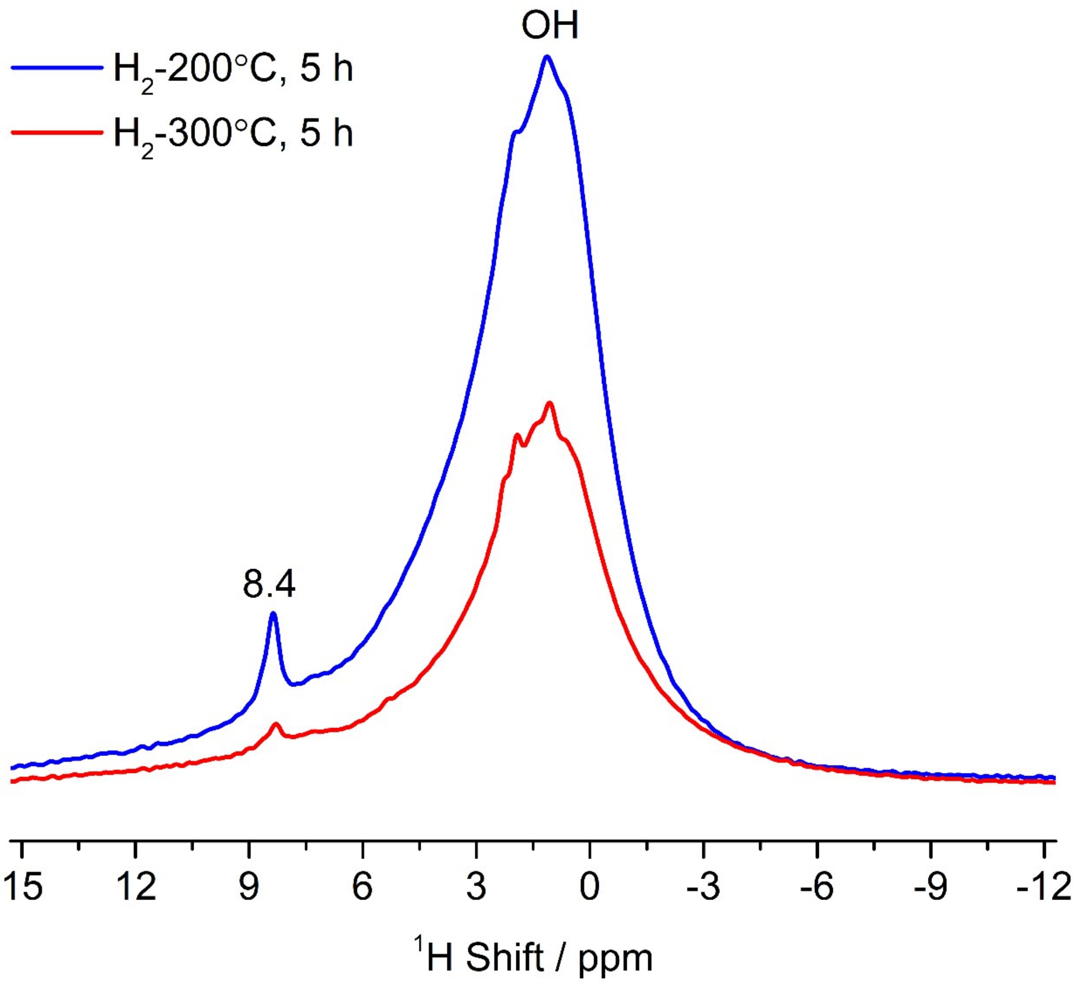

Fig. S12 ^{1}H MAS NMR spectra of ZnO nanorods after exposing to H_2 (500 mbar) at 200 °C and 300 °C, respectively.

8. References

1 L. Lin, Y. Yang, L. Men, X. Wang, D. He, Y. Chai, B. Zhao, S. Ghoshroy and Q. Tang, *Nanoscale* 2013, **5**, 588−593.

2 B. Song, Y. Li, X. Wu, F. Wang, M. Lin, Y. Sun, A. Jia, X. Ning, L. Jin, X. Ke, Z. Yu, G. Yang, W. Hou, W. Ding, X. Gong and L. Peng, *J. Am. Chem. Soc.*, 2022, **144**, 23340–23351.

3 V. Ischenko, S. Polarz, D. Grote, V. Stavarache, K. Fink and M. Driess, *Adv. Funct. Mater.*, 2005, **15**, 1945–1954.